Master Sciences de la matière
École Normale Supérieure de Lyon
Université Claude Bernard Lyon I

Stage 2018–2019
Lisa Blum Moyse
M1 Physique

A stochastic model for heterogeneous reactions: the case of enzymatic mineralisation

Abstract: This research project aims at modelling the aggregation process between bacteria, in order to characterise a reaction these microbes catalyse: the oxidation of manganese (Mn). For that purpose we use the deterministic and mean-field Becker-Döring and Smoluchowski equations which model coagulation processes. Starting from an experimental distribution of microbial clusters sizes, we seek to model these data by determining suitable aggregation kernels. We also consider the effect of microbial growth by developing a logistic model for bacterial clusters. Finally, we apply the appropriate coagulation equations to model the kinetics of Mn oxidation.

Key words: *Aggregation, Stochastic models, Smoluchowski, Becker-Döring, Logistic model.*

Internship supervised by:
Pietro de Anna, Duccio Fanelli, Franco Bagnoli
Pietro.DeAnna@unil.ch, duccio.fanelli@unifi.it, franco.bagnoli@unifi.it /
tel. 055 4572336
Department of Physics and Astronomy
Via Giovanni Sansone, 1, 50019 Sesto Fiorentino (Firenze), Italy
https://www.fisica.unifi.it/

August 4, 2019

Acknowledgements

I thank Pietro de Anna and Duccio Fanelli for their mentoring and investment all along the research project, Franco Bagnoli for welcoming me in this lab. Thank you to all the members of the team for their sympathy.

Contents

Nomenclature

General

C_r Cluster of r bacteria

c_r Concentration of clusters of r bacteria

M Mass of bacteria

n_c Maximum cluster's size

r Number of bacteria constituting an aggregate, or volume

Becker-Döring model

a_r Aggregation rate or kernel between clusters C_r and C_1

b_r Fragmentation rate or kernel of a cluster C_{r+1}

J_r Net mass flux from C_r and C_1 to C_{r+1}

Smoluchowski model

$a_{r,s}$ Aggregation rate or kernel between clusters C_r and C_s

t_g Gelation time

Microbial growth

A_r Aggregation terms

K Growth rate of bacteria

M_∞ Carrying capacity of a bacterial system

Kinetics of Mn

c_M Concentration of manganese (Mn)

K_m Reaction rate constant of oxidation of manganese (Mn)

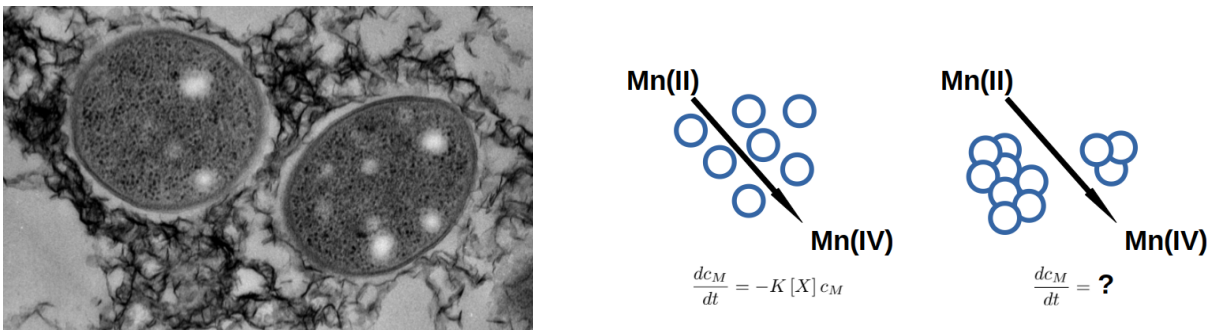

(a) (b)

Figure 1: (a) Picture made with an electronic microscope (curtesy of Prof. Jasquelin Pena) showing two bacteria, P. Putida, and precipitated Mn (black filaments). (b) The oxidation of manganese (Mn) transforms Mn with an oxidation number equal to II in Mn(IV). This reaction can be catalysed by bacteria (blue circles). In case of separated bacteria (monomers) the kinetics is known, described as a first order reaction. Nevertheless in case of bacteria aggregated in clusters, the latter kinetics remains to be determined.

1 Introduction

Dissolved minerals under certain conditions can precipitate into solid particles, a process called mineralisation. In some situation the kinetics of this process can be boosted by orders of magnitude by the presence of microorganisms that act as enzymes to catalyse the reaction. The case of enzymatic mineralisation of manganese (Mn) has received attention due to the role played by the extremely reactive Mn oxides in natural phenomena, including several elements cycle. The enzymatic mineralisation of suspended Mn by microbial activity, involves entities of different size: suspended Mn molecules (molecule scale) and microbes (micron scale and above). The latter also aggregate to shape microbial clusters that diffuse, sediment, collide with other clusters and react with dissolved Mn (see Fig. 1). This complex phenomenon is typically described in terms of first order kinetics that, while providing a simple framework depending on bulk concentrations and chemical conditions (like pH), does not take into consideration the microscopic process of microbial aggregation that probably control the overall reaction kinetics.

This research project aims at developing a novel stochastic model that takes into account the dynamics associated to the aggregates formation and the microbial growth of bacteria, to finally explain its impact on the overall reaction kinetics. For that purpose we start from results of an experiment measuring different bacterial clusters sizes. We aim at modelling the obtained experimental size distribution by using suitable aggregation models. The proposed models, consist in a set of chemical equations that describe

- The interaction between microbes and microbial aggregates with dissolved Mn.
- The microbes interactions to build microbial aggregates.

The system state will be described in terms of the population of all involved species and its dynamics in terms of transitions associated to the defined mechanisms. Thus, the system state will be distributed as the solution of a system of differential equations that is set in terms of the reaction kinetics associated to the Mn microbes interactions and the microbial aggregates formation.

There are many approaches to model the phenomenon of aggregation between particles. Here we will use the deterministic (mean-field) and discrete models of Smoluchowski and Becker-Döring [1].

We model the aggregation between two clusters of size r and s, which leads to a cluster of size r+s, and also the fragmentation of this cluster into two smaller ones (see eq. (1) and Fig. 2).

$$C_r + C_s \rightleftharpoons C_{r+s} \tag{1}$$

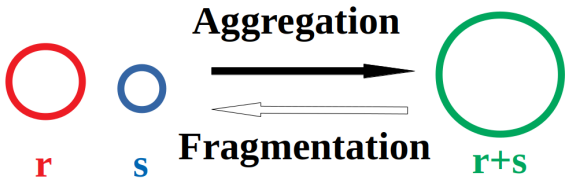

Figure 2: Diagram showing aggregation and fragmentation processes. The aggregation process between two particles of respective sizes r and s, corresponding to the number of monomers constituting of the cluster, leads to a cluster of size $r + s$. Inversely the fragmentation process splits the whole cluster of size $r + s$ into two smaller clusters r and s.

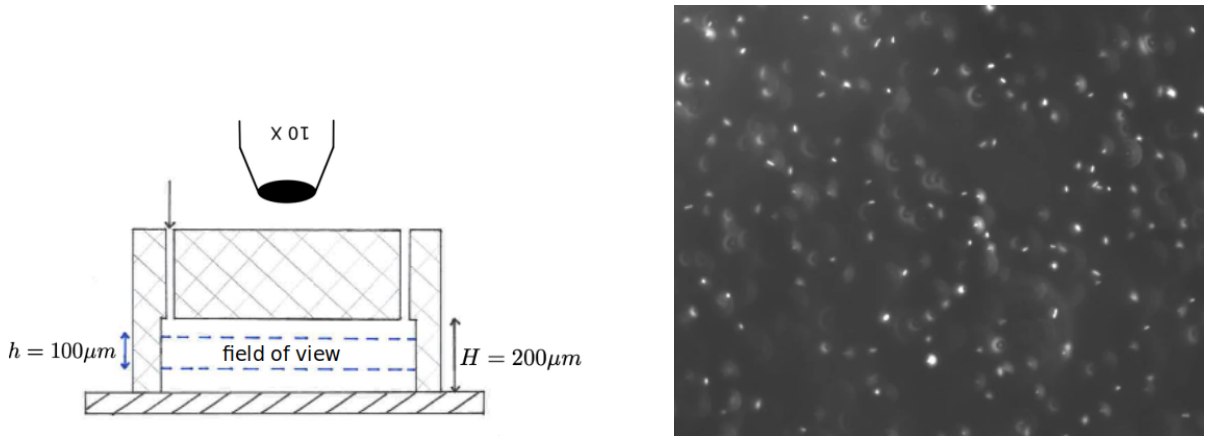

(a) (b)

Figure 3: Experiment highlighting bacterial clustering. (a) Experimental setup: a solution of separated bacteria (monomers) is injected into the channel at a time $t = 0$. Bacteria stay in suspension. After 16 hours pictures are made with an optical microscope, which has access to a limited field of view. (b) Resulting picture. White spots correspond to bacteria or clusters of bacteria.

Firstly we present the obtained experimental results that we will to model. Secondly we will discuss a first mathematical model of aggregation, the Becker-Döring equations. Then, we will consider a second model that takes into consideration more physical processes, resulting complicated to solve: the Smoluchowski equations. Since the considered particles are bacteria, we complete the model by adding the phenomenon of microbial growth. Finally we use a suitable coagulation model to study the impact on the kinetics of the mineralisation of Mn mediated by microbial aggregates.

2 Experimental distribution of bacterial clusters sizes

2.1 Setup and measurements

The following experiment was carried out by Filippo Miele at the University of Lausanne, its aim was to observe bacterial aggregates of different sizes. Pseudomonas putida sp. from a frozen stock were grown in LB medium at 29 degrees for 18 hours, in an orbital shaker at 150 rpm. Then, 10 samples of 100 uL were injected into 10 microfluidic straight channels (see Fig. 3). Observations were made with an optical microscope in phase contrast optical configuration, and a picture for each sample was acquired.

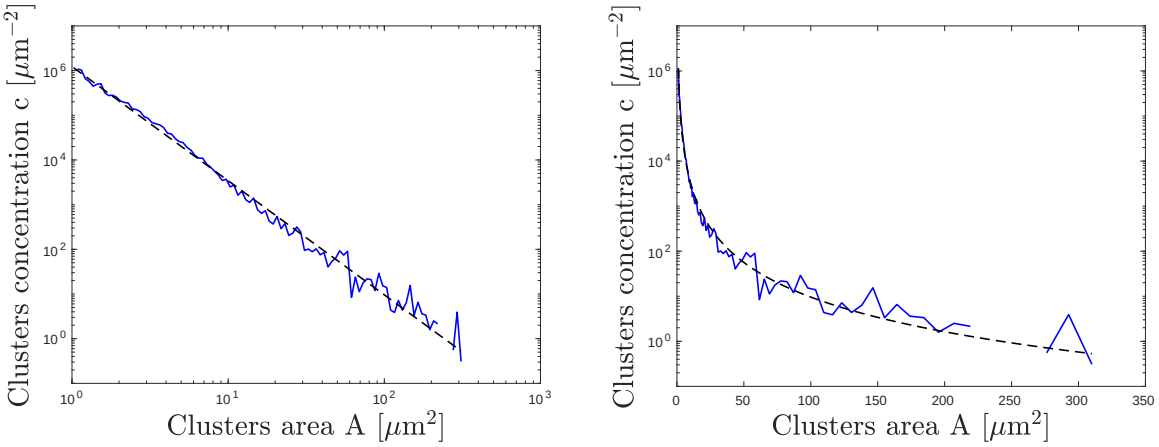

(a) log-log scale (b) semi-log scale

Figure 4: Averaged concentrations distribution of clusters areas $c(A)$ (10 measurements) of bacterial clusters areas A, plotted with a log-log scale (a) or a semi-log scale (b) in order to discriminate a potential power or exponential law. The black dashed line is a fit which corresponds to a power law $A^{-\alpha_A}$, with $\alpha_A = 2.55$.

2.2 Analysis of the resulting pictures: obtention of a clusters sizes distribution

Starting from these pictures, a script detects and measures the area A of every cluster. The result is a list of areas values. We then compute the probability density function (PDF) $p(A)$ of these data, which corresponds to the the density of probability to get a measurement between the A and $A + dA$. For that purpose we compute the frequency of occurrence of the latter data values. In a spatially extended system:

$$p(A) =< \delta(A - A') > \sim \int_{A_{tot}} dA' \; c(A')\delta(A - A') = c(A) \tag{2}$$

Where angular brackets represents surface averaging and $c(A)$ is the cluster of area A concentration, which, therefore, coincides with the defined PDF.
The obtained concentration distribution $c(A)$ is not linear (see Fig. 4).

In order to determine whether this distribution follows a power or an exponential law, we plot the distribution versus the clusters size with a semi-log or log-log scale. If the experimental points are distributed as a straight line in semi-log scale (resp. log-log scale) this means that the distribution follows an exponential law (resp. power law). In fact the collected data display a power law decay with the characteristic exponent $\boxed{\alpha_A = 2.55}$.

In the further parts of this report we will mainly use a concentrations distribution of clusters as a function of volume. We name r the number of bacteria constituting a cluster, and consider an elementary volume of one bacteria $V_0 = 1\ \mu m$. So we get the volume of a cluster of size r: $V_r = rV_0 = r$. From now on we will refer to r as to the volume of a cluster of r monomers. Since the further investigations rely on numerical models, we will use arbitrary units.

Starting from the concentration distribution as a function of the area A ($c(A)$), the plot of c as a function of the volume r ($c(r)$) and the radius R ($c(R)$) is obtained via the change of variables: $c(X) = c(A)\frac{dA}{dX}$, where X refers either to the volume r or the radius R. The derivative $\frac{dA}{dX}$ is calculated by assuming a spherical shape for the aggregates, that is:

$$\left\{ \begin{array}{l} A = 4\pi R^2 \\ r = \frac{4}{3}\pi R^3 \end{array} \right. \Longrightarrow \left\{ \begin{array}{c} R \sim r^{1/3} \\ A \sim R^2 \sim r^{2/3} \end{array} \right. \tag{3}$$

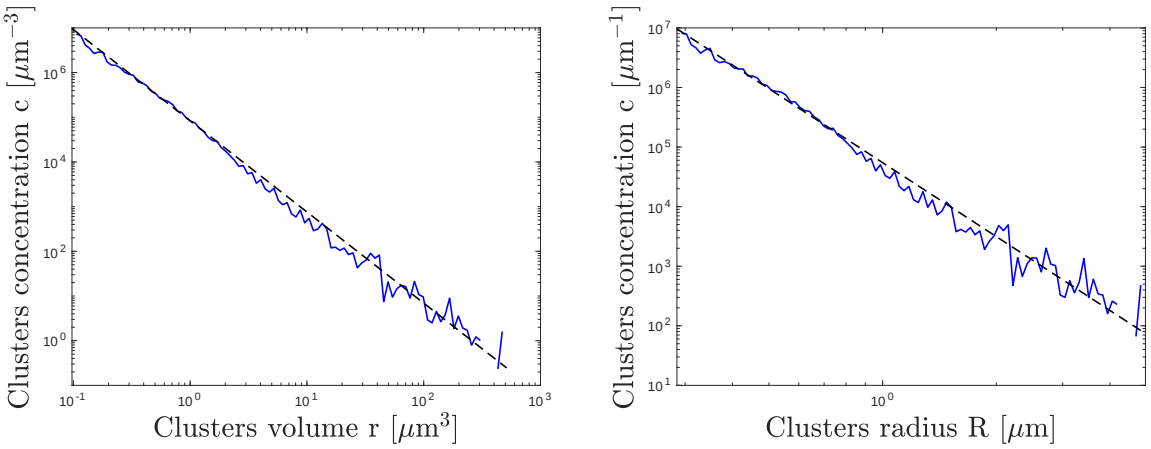

(a) (b)

Figure 5: Averaged concentrations distribution of clusters c (10 measurements) as a function of the volume r (a) or the radius R (b) of bacterial clusters. The black dashed lines are fits which correspond to power laws $r^{-\alpha_r}$, $\alpha_r \sim 2$ and $R^{-\alpha_R}$, $\alpha_R \sim 4$.

Assuming $c(A) \sim A^{-\alpha_A}$ we get for c(r):

$$c(r) = c(A)\frac{dA}{dr} \sim (r^{2/3})^{-\alpha_A} r^{-1/3} \sim r^{-(1/3)(\alpha_A+1)} \sim r^{-\alpha_r} \tag{4}$$

Similarly we get $c(R) \sim R^{-2\alpha_A+1} \sim R^{-\alpha_R}$. The numerical application with $\alpha_A = 2.55$ involves $\alpha_r \sim 2$ and $\alpha_R \sim 4$. The results are presented in Fig. 5. From now on we write $c(A) := c_A$, $c(r) := c_r$ to simplify notations. Finally the distribution we will seek to model in this project is the power law which follows $\boxed{c_r \sim r^{-\alpha_r} \sim r^{-2}}$. In order to understand the underlying mechanisms for the formation of these microbial aggregates, we will study, implement and develop some aggregation-fragmentation models.

Let us move onto a first model which builds on the celebrated Becker-Döring equations [1]. This simplified model allows a first approach of coagulation processes and eases analytical calculations.

3 A simplified model for analytical studies: Becker-Döring aggregation-fragmentation equations

3.1 Formulation

According to the Becker-Döring equations, the loss or gain of a single particle at a given time takes place [1] (with respect to the schematic of Fig. 2, $s = 1$):

$$C_r + C_1 \rightleftharpoons C_{r+1} \tag{5}$$

where C_r denotes a cluster composed of r fundamental units.

Remark: The Becker-Döring and Smoluchowski equations (as we will see) are typically considered for an infinite maximum cluster's size $n_c \to \infty$. Nevertheless we consider in this project a finite maximum cluster's size n_c, both for physical reasons (bacterial clusters can not have an infinite size because of space and food supplies) and numerical reasons (the implementation requires limits).

If the clustering occurs with an aggregation rate a_r and fragmentation rate b_{r+1} (also referred as aggregation and fragmentation kernels), and c_r denotes the concentration at time t of clusters C_r, the

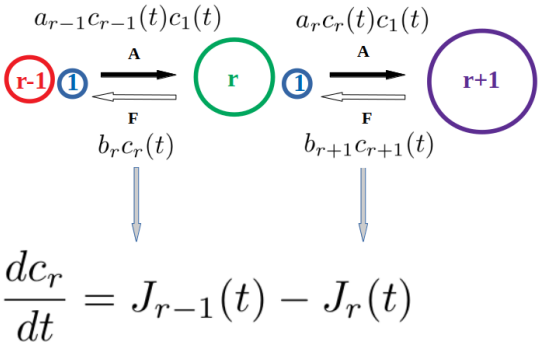

Figure 6: Diagram showing the physical meaning of each term of the Becker-Döring equations. A and F refer to respectively the aggregation and fragmentation processes. The aggregation process is represented from left to right: a cluster C_{r-1} and a monomer (one bacteria) C_1 can coagulate to form a cluster C_r, which also can aggregate with an other monomer to become a cluster C_{r+1}. Similarly, the fragmentation process is represented from right to left. $c_r(t)$ refers to the concentration of clusters of r monomers. a_r and b_r are respectively the aggregation and fragmentation rates. $J_{r-1}(t)$ is the net rate at which clusters of size r are created from clusters of size $r-1$, and $J_r(t)$ is the net rate at which clusters of size $r+1$ are created from clusters of size r. The variation of $c_r(t)$ is a balance between processes which increase or decrease the concentration of clusters of size r.

law of mass action yields for the concentrations $\{c_r(t)\}_{r=2}^{n_c}$ the equations:

$$\frac{dc_r}{dt} = J_{r-1}(t) - J_r(t) \qquad (r \geq 2) \tag{6}$$

Where the fluxes $J_r(t)$ are defined by

$$J_r(t) = a_r c_r(t)c_1(t) - b_{r+1}c_{r+1}(t) \tag{7}$$

This quantity is the net rate at which clusters of size $r+1$ are created from clusters of size r. The Fig. 6 sums up the meaning of each term of the equations. $J_{r-1}(t)$ stems from the aggregation-fragmentation process which forms or splits a cluster of volume r. This corresponds to the process:

$$C_{r-1} + C_1 \rightleftharpoons C_r \tag{8}$$

$J_r(t)$ corresponds to the aggregation-fragmentation process which forms or splits a cluster of volume $r+1$. This originates from the process:

$$C_r + C_1 \rightleftharpoons C_{r+1} \tag{9}$$

The total mass of the system is defined as:

$$M(t) = \sum_{r=1}^{n_c} r c_r(t) \tag{10}$$

We here impose the mass conservation $M(t) = M_0$, where M_0 is the initial mass of separated bacteria (monomers), with the condition on the mass of monomers:

$$M_1(t) = c_1(t) = M_0 - \sum_{r=2}^{n_c} r c_r(t) \tag{11}$$

We first implement the model and test it for already known analytical solutions, in order to verify a coherence between mathematical developments and numerical implementation.

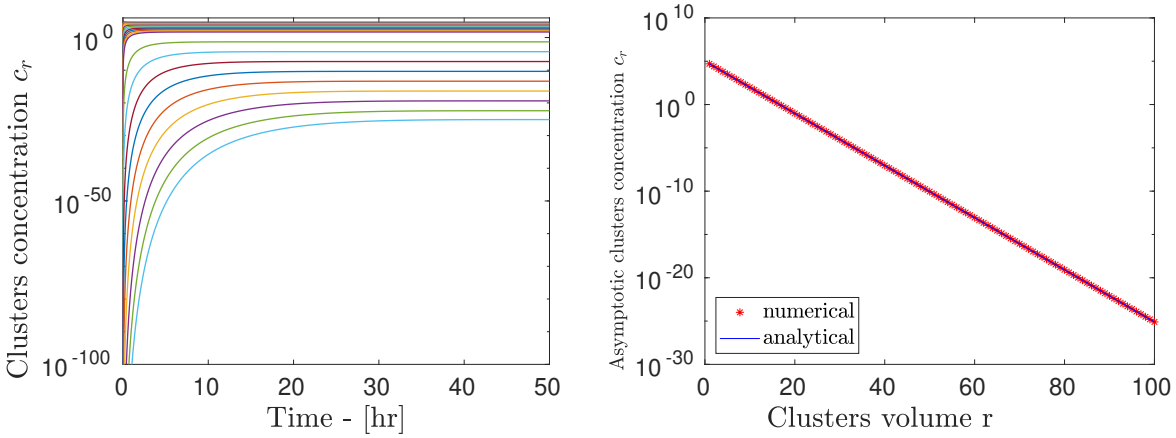

(a) (b)

Figure 7: Numerical simulation of the Becker-Döring model with constant kernels $a_{r,s} = a_0$, $b_{r,s} = b_0$. (a) Temporal evolution of each cluster's size, represented by a different line's colour. The final state is an equilibrium state. (b) Asymptotic clusters concentration c_r. The red dots correspond to numerical values, the blue line corresponds to the analytical solution (see eq. (12)). Furthermore the straight behaviour with the semi-log scale highlights that c_r follows an exponential law.

3.2 Implementation of an analytical solution for constant kernels, $a_r = a_0$, $b_r = b_0$

Ideally, the aim is to solve explicitly the system of ordinary differential equations. However for many physically relevant aggregation and fragmentation rates a_r and b_r the system is too complicated. Nevertheless we can study if there is convergence to an equilibrium or a steady-state.

Remark: The term 'steady-state' corresponds to $J_r = J_{r-1}$, while 'Equilibrium' refers to $J_r = 0$ for each r. In this research project, in order to discriminate for numerical results whether a state is equilibrium or steady-state, we compare the minimum of $\frac{dc_r}{dt}$ and J_r with a threshold value ϵ. If the condition $\min(\frac{dc_r}{dt}, J) < \epsilon$ is satisfied, that means that the state would be at equilibrium ($\min = J_r$) or steady ($\min = \frac{dc_r}{dt}$).

For a simple case we consider the following conditions: equilibrium state and $a_r = a_0$, $b_r = b_0$ constants.

The known solution [1] is written:

$$c_{eq,r} = \left(\frac{ac_1}{b}\right)^{r-1} c_1 := \theta^{r-1} c_1 \tag{12}$$

with

$$c_1 = \frac{A - \sqrt{A^2 - 4BM}}{2B} \tag{13}$$

$$A = 1 + 2a/bM;\ B = \frac{a^2}{b^2} \tag{14}$$

$\theta = \frac{ac_1}{b}$ is a useful measure of the relative strength of aggregation to fragmentation. If $\theta < 1$ fragmentation dominates aggregation, and inversely. Furthermore $c_{eq,r}$ converges if $\theta < 1$.

Remark: The used computational language matlab is affected by numerical error for values below 10^{-15}. In this case the distribution decays exponentially and so achieves very small values. In order to be sure that there is no artefact due to this numerical limit, we fixed initial conditions $c(t = 0)$ larger enough for the script, and then scale again for plots. This justifies the small values displayed on

Fig. 7, 11.

After a transition regime, the system achieves an equilibrium state (Fig. 7). The numerical implementation well reproduces the analytical solution (exponential law, see eq. (12)) provided the consistency of a_r, b_r and the condition $\theta = \frac{ac_1}{b} < 1$. By this way we have checked that the model has been correctly implemented.

Nevertheless the experimental data display not an exponential but a power law $c_r \sim r^{-2}$.
We will now study analytically the Becker-Döring equations in order to determine which conditions could allow to get the power law distribution we are looking for.

3.3 Developments: Becker-Döring analytical solutions

3.3.1 Analytical kernels a_r, b_r to get $c_r \sim r^{-\alpha}$ for a steady-state:

In the case of the system being in a steady-state, that is $\frac{dc_r}{dt} = 0$, we are search what kind of aggregation-fragmentation rates a_r, b_r could involve $c_r = c_1 r^{-\alpha}$ (steady-state solution), where α is a general power. The Becker-Döring equations (eq. (6)) imply $\forall r \geq 2$:

$$\frac{dc_r}{dt} = 0 \Leftrightarrow J_{r-1} = J_r \Leftrightarrow a_r c_1 c_r - b_{r+1} c_{r+1} = a_{r-1} c_1 c_{r-1} - b_r c_r \tag{15}$$

$$\Longleftrightarrow a_r c_1 r^{-\alpha} - b_{r+1}(r+1)^{-\alpha} = a_{r-1} c_1 (r-1)^{-\alpha} - b_r r^{-\alpha} \tag{16}$$

One trivial solution of this equation would be:

$$\begin{cases} a_r = \frac{a_0}{c_1} r^{\alpha} \\ b_r = b_0 r^{\alpha} \end{cases} \tag{17}$$

with a_0, b_0 are arbitrary constants. Furthermore c_1 can be determined invoking mass conservation condition:

$$c_1 = M_0 - \sum_{r=2}^{n_c} r c_r = M_0 - c_1 \sum_{r=2}^{n_c} r^{1-\alpha} \tag{18}$$

$$\Longleftrightarrow c_1 = M_0 \left(1 + \sum_{r=2}^{n_c} r^{1-\alpha} \right)^{-1} \tag{19}$$

We test numerically this analytical solution (see Fig. 8). The numerical results correspond to the expected solution. Nevertheless this solution is only one possibility which satisfies our conditions. We will then search a general solution for c_r for such kernels a_r, b_r in the more restrictive case of an equilibrium state.

3.3.2 General solutions for equilibrium, kernel $a_r = a_0 r^{\alpha}$, $b_r = b_0 r^{\alpha}$

We seek to determine c_r for kernels $a_r = a_0 r^{\alpha}$, $b_r = b_0 r^{\alpha}$.

Calculation with perturbation: At equilibrium, $\forall r \geq 2$, $J_r = 0$ (consequently $c_1(t)$ is constant). Furthermore we consider $a_r = a_0 r^{\alpha}$, $b_r = b_0 r^{\alpha}$. So we get:

$$J_r = 0 = a_0 r^{\alpha} c_r c_1 - b_0 (r+1)^{\alpha} c_{r+1} \Longleftrightarrow \frac{c_{r+1}}{c_r} = \frac{a_0 c_1}{b_0} \left(\frac{r}{r+1} \right)^{\alpha} \tag{20}$$

We write $\theta = \frac{a_0 c_1}{b_0}$. By setting $c_{r+1} \sim c_r + c'_r$, where c'_r is a small perturbation, we have:

$$\frac{c'_r}{c_r} = \theta \left(\frac{r}{r+1} \right)^{\alpha} - 1 = \theta \left(\frac{1}{1+\frac{1}{r}} \right)^{\alpha} - 1 \sim \theta \left(1 - \frac{\alpha}{r} \right) - 1 \tag{21}$$

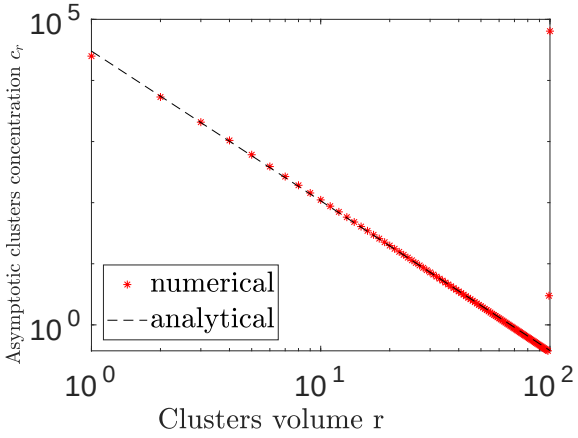

Figure 8: Numerical simulation of the Becker-Döring model for a steady-state with kernels $a_r = \frac{a_0}{c_1} r^\alpha$, $b_r = b_0 r^\alpha$. Asymptotic clusters concentrations and analytical solution $c_r = M_0 \left(1 + \sum_{r=2}^{n_c} r^{1-\alpha}\right)^{-1} r^{-\alpha}$ (dashed black line).

thanks to a Taylor expansion ($r \gg 1$). After integration (continuous limit):

$$\ln\left(\frac{c_r}{c_1}\right) = (\theta-1)(r-1) - \alpha\theta \ln(r) \text{ and finally: } c_r = c_1 e^{(\theta-1)(r-1)} r^{-\alpha\theta} = \boxed{\kappa_1 r^{-\alpha\theta} e^{(\theta-1)r}} (*) \quad (22)$$

$$\text{Where } \kappa_1 = c_1 e^{1-\theta} \quad (23)$$

We here recognise the expression of a Gamma distribution: $\frac{1}{\Gamma(k)\phi^k} r^{k-1} e^{-\frac{r}{\phi}}$. By identification:

$$\begin{cases} \frac{1}{\Gamma(k)\phi^k} = c_1 e^{\theta-1} \\ \\ k-1 = -\alpha\theta \\ \frac{1}{\phi} = 1-\theta \end{cases} \quad (24)$$

It is possible to determine numerically c_1. In fact the eq. (**??**) is a self-consistent equation. If we define a function $f(x) = x - M_0 - \sum_{r=2}^{n_c} r c_r$, we can search for which values x we get $f(x) = 0$, since c_1 should satisfy $f(x) = 0$.

Solution with a test function: As an exercise we can also substitute the expression of the Gamma distribution directly at the step just before the approximation, that is:

$$\frac{c_{r+1}}{c_r} = \theta \left(\frac{r}{r+1}\right)^\alpha \implies \frac{(r+1)^{k-1} e^{-\frac{r+1}{\phi}}}{r^{k-1} e^{-\frac{r}{\phi}}} = \left(\frac{r+1}{r}\right)^{k-1} e^{-\frac{1}{\phi}} := \theta \left(\frac{r}{r+1}\right)^\alpha \quad (25)$$

So by identification, one possibility is:

$$\begin{cases} k-1 = -\alpha \\ \frac{1}{\phi} = -\ln(\theta) \end{cases} \quad (26)$$

So an other solution using this test function but without approximation would be:

$$c_r = \frac{1}{\Gamma(k)\phi^k} r^{k-1} e^{-r/\phi} = \frac{1}{\Gamma(1-\alpha)} (-\ln(\theta))^{1-\alpha} r^{-\alpha} e^{r\ln(\theta)} = \boxed{\kappa_2 r^{-\alpha} \theta^r} (**) \quad (27)$$

$$\text{with } \kappa_2 = \frac{1}{\Gamma(1-\alpha)} (-\ln(\theta))^{1-\alpha} \quad (28)$$

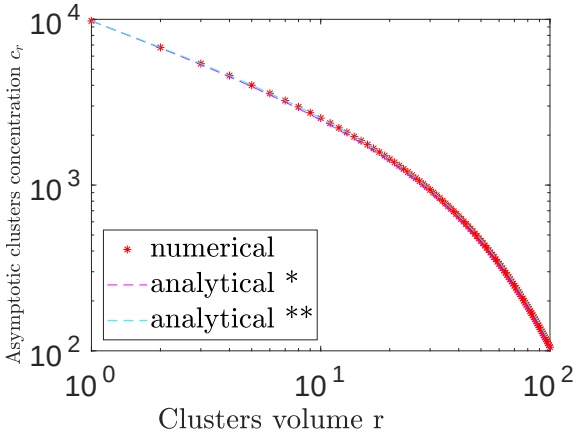

Figure 9: Numerical simulation of the Becker-Döring model with kernels $a_r = a_0 r^\alpha$, $b_r = b_0 r^\alpha$. Asymptotic clusters concentrations c_r and analytical solutions (dashed magenta and blue lines), for $\alpha = 0.5$. The asymptotic state is an equilibrium state. The numerical values follow both analytical solutions, corresponding to a Gamma distribution.

We have the following conditions on the Gamma distribution parameters [8]:

$$\begin{cases} k > 0 \Longleftrightarrow \alpha < 1 \\ \phi > 0 \Longleftrightarrow \theta < 1 \end{cases} \tag{29}$$

Interestingly we retrieve the fact that the ratio between aggregation and fragmentation should respect $\theta < 1$ to achieve an equilibrium state.

If we want to find c_1 analytically we have:

$$c_1 = \frac{(-1)^{\alpha-1}}{\Gamma(1-\alpha)} \ln\left(\frac{a_0 c_1}{b_0}\right) \frac{a_0 c_1}{b_0} \Longleftrightarrow c_1 = \frac{b_0}{a_0} exp\left(-(\Gamma(1-\alpha)\frac{b_0}{a_0})^{\frac{1}{1-\alpha}}\right) \tag{30}$$

We then test numerically these analytical results (see Fig. 9).

The numerical values follow both analytical solutions, corresponding to a Gamma distribution.

Apart from microbial clustering, it is interesting to point out the fact that such Gamma distributions are observed for distributions of the size of pores in porous media. So we could propose the Becker-Döring model with kernels $a_r = a_0 r^\alpha$, $b_r = b_0 r^\alpha$ to be an explanation for the formation of porous media, substituting bacteria with typical grains. This hypothesis is physically consistent in the sense that porous media would be formed by a progressive input of elementary particles, thus justifying the loss or gain of a single particle in each aggregation-fragmentation process.

Even if the Becker-Döring model yields a somehow artificial power law distribution for clusters sizes, as the one we search, it is too simplified and does not reflect the real physical process that is at play in the scrutinised sample. In fact aggregation can also take place between clusters of different sizes. Furthermore we have so far considered also the fragmentation process, which is unlikely to happen in case of formation of microbial aggregates. Once bacteria are aggregated in a cluster, they do not split. That is why we now move onto a second set of equations to describe the aggregation process between bacteria: the Smoluchowski model.

4 Smoluchowski coagulation equations

Smoluchowski coagulation equation describes the kinetics of the process of binary aggregation. Consider a well-stirred vessel in which clusters of a variety of sizes move about and occasionally collide

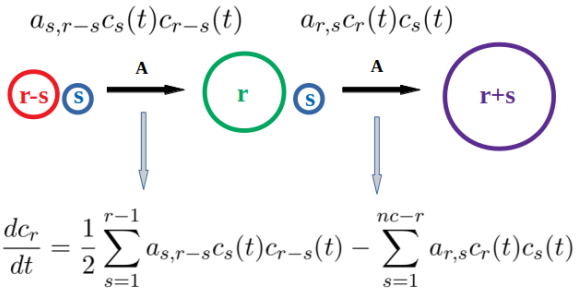

Figure 10: Diagram showing the physical meaning of each term of the Smoluchowski equations. A refers to the aggregation process. The aggregation process is represented from left to right: two clusters C_{r-s} and C_s can coagulate to form a cluster C_r, which also can aggregate with an other cluster of size s, C_s, to become a cluster C_{r+s}. $c_r(t)$ refers to the concentration of clusters of r monomers. a_r is the aggregation rate, or kernel. The first sum corresponds to all the aggregation processes which form a cluster of volume r. The second sum corresponds to all the aggregation processes which form a cluster of volume $r+s$. The variation of $c_r(t)$ is a balance between processes which increase or decrease the concentration of clusters of size r.

and coalesce with each other. A set of differential equations models how the cluster-size distribution changes over time.

4.1 Formulation

The process of aggregation between two clusters C_r and C_s,respectively composed of r and s fundamental units, obeys:

$$C_r + C_s \rightarrow C_{r+s} \qquad \forall\ r, s \geq 1 \tag{31}$$

We here consider only binary fragmentation. We denote the aggregation rate by $a_{r,s}$, also referred as "aggregation kernel" or simply "kernel". We apply the law of mass action, which yields the equations (for n_c the maximum cluster's size):

$$\frac{dc_r}{dt} = \frac{1}{2}\sum_{s=1}^{r-1} a_{s,r-s}c_s(t)c_{r-s}(t) - \sum_{s=1}^{n_c-r} a_{r,s}c_r(t)c_s(t) \qquad (r \geq 2) \tag{32}$$

We get the equation for the monomer concentration by ignoring the first sum in eq. (32).

$$\frac{dc_1}{dt} = -\sum_{s=1}^{n_c-1} a_{1,s}c_1(t)c_s(t) \tag{33}$$

Remark: In case of a finite maximum cluster's size n_c, these equations conserve the mass.

Fig. 10 sums up the meaning of each term of the equations. The first sum corresponds to all the aggregation processes which form a cluster of volume r. This corresponds to the process:

$$C_{r-s} + C_s \rightarrow C_r \tag{34}$$

The 1/2 factor allows to correct for the double counting of the first sum.

The second sum corresponds to all the aggregation processes which form a cluster of volume $r+s$. This corresponds to the process:

$$C_r + C_s \rightarrow C_{r+s} \tag{35}$$

4.2 Implementation of an analytical solution

A solution for the Smoluchowski equations is, in general, not known. However in some special cases, they admit analytical solutions [1].

Multiplicative kernel: $a_{r,s} = rs$**.** Here we focus on an analytical power law distribution $c_r \sim r^{-5/2}$, which could well model the experimental data. The theoretical expressions for such kernel are [1]:

$$c_r(t) \sim \begin{cases} \frac{e^{-r(t-1-log(t))}}{r^{5/2}t\sqrt{2\pi}} & t < t_g = 1 \\ \frac{1}{r^{5/2}t\sqrt{2\pi}} & t \geq t_g = 1 \end{cases} \tag{36}$$

Where t_g is the gelation time, which corresponds in the case of an infinite maximum cluster size $n_c \to \infty$ to the earliest moment where conservation of the total mass fails: $t_g := \inf\{t > 0 : M(t) < M(0)\}$. In our case where n_c is a finite number, we set:

$$M'(t) = \sum_{r=1}^{n_c-1} rc_r(t) \tag{37}$$

and consider that the definition of t_g occurs for M'. In fact for a finite size system the mass does not go to infinity but in the biggest cluster size class C_{nc}.

The numerical results are consistent with the expected calculations (see Fig. 11). The obtained distribution follows $c_r \sim r^{-5/2}$, where r represents the volume. If this model was supposed to explain the experimental data, $c_A \sim A^{-5/2}$, it would mean that the aggregates had a flat shape, like the section of a cylinder, so that $A \sim r$ (see Fig. 12).

We have so far considered a fixed number of bacteria, that is a constant mass $M(t) = M_0$. Nevertheless bacteria are not passive particles and grow when they are in a suitable environment, which is the case in the previously described experiment (see section 2).

4.3 Developments: Smoluchowski model and microbial growth

4.3.1 Classical logistic model for bacteria (monomers)

The model has been incomplete so far, since it has not taken into account the ability of bacteria to multiply, which is observed in the considered experiment. In fact in case of non-aggregated bacteria the growth of a bacterial population obeys the logistic model [9] (see Fig. 13). Here we do not take into account the death phase, since this has not been observed in the experiment we consider. In case of non-aggregated bacteria (monomers) the logistic model thus obeys the following law:

$$\frac{dM}{dt} = KM(t)\left(1 - \frac{M(t)}{M_\infty}\right) \tag{38}$$

Where M denotes the mass of bacteria, K the growth rate, which is the inverse of the doubling time $t_d = 1/K$, which is the characteristic time at which all bacteria divide. M_∞ is the carrying capacity of the system, or the maximum biomass that the system can sustain: once it is reached, the growth stops due to depletion of nutrients and space availability.

4.3.2 Logistic model for bacterial clusters: first equations (growth of a whole cluster)

In the context of coagulation between bacteria, we have to modify the form of this logistic model, in order to take into account the binary division of individual cells for every cluster's class. We propose the following equations, with A_r corresponding to the aggregation terms previously described (see

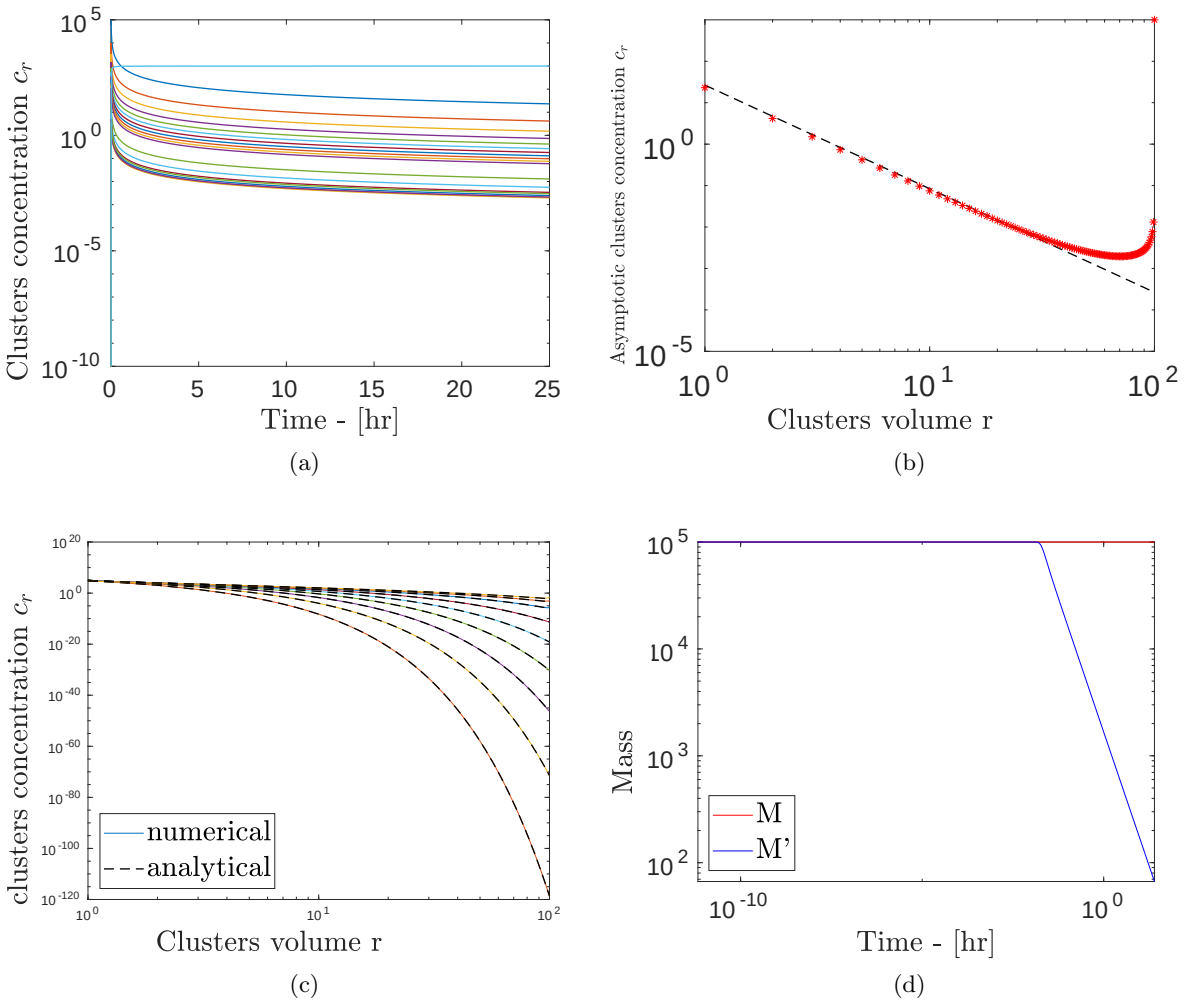

Figure 11: Numerical simulation of the Smoluchowski model with kernel $a_{r,s} = rs$. (a) Temporal evolution of each cluster's size, (b) Asymptotic clusters concentration c_r and analytical solution (dashed black line), (c) Temporal evolution of the clusters concentration c_r, and corresponding analytical solutions (dashed black lines), (d) Temporal evolution of the total mass (M) and mass excepted for the maximum cluster's size n_c (M'). The expected analytical decay at the gelation time t_g occurs for M' and not M, due to the finite size of the simulation.

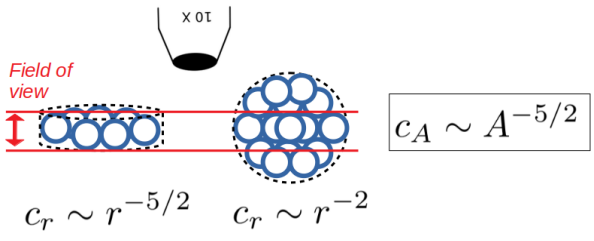

Figure 12: Diagram illustrating the meaning of distributions laws. We know that $c_A \sim A^{-5/2}$. The distribution of clusters volumes c_r depends on the shape of aggregates (due to the relation between the area A and the volume r). If aggregates had a flat shape (left side), it would mean that the area A has the same dependence than the volume r, which involves $c_r \sim r^{-5/2}$ (as we studied in this section). On the opposite if aggregates had a spherical shape (right side), it would mean that the dependence is $A \sim r^{2/3}$, which involves $c_r \sim r^{-2}$ (see section 2). The experiment does not allow to distinguish the two possibilities, since measurements are made with a microscope which has access to a limited plane field of view.

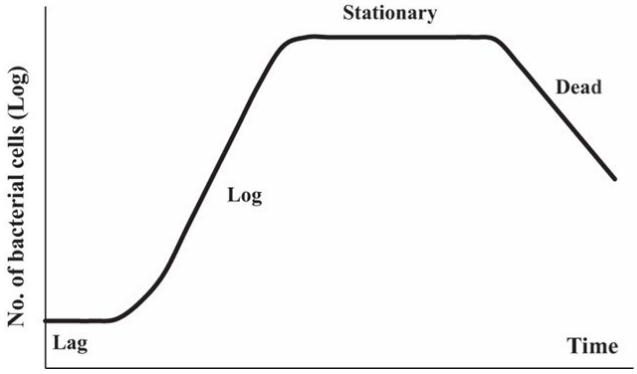

Figure 13: Logistic model modelling bacterial growth (in classical case of separated bacteria). When bacteria are injected in a suitable medium, after a latency period they multiply until a maximum value (stationary state) and finally die because of the lack of nutrients.

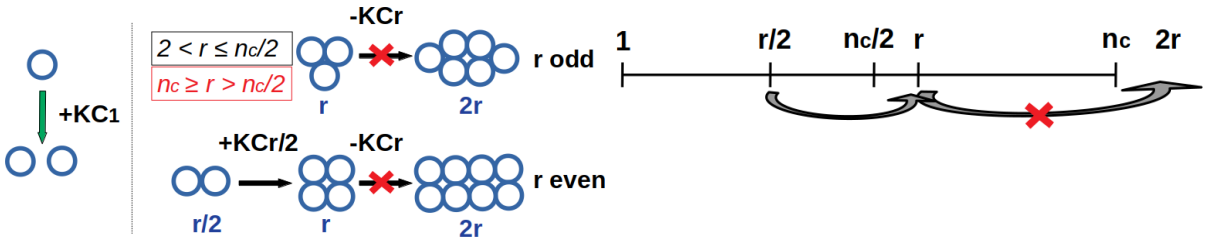

(a) (b)

Figure 14: (a) Diagram illustrating the growth for each case. For monomers (left side), a bacterium divides and leads to two separated bacteria. Right side: If $r \leq n_c/2$, there are two possibilities: If the number of bacteria r of a cluster is odd (top) it is only possible for it to grow, becoming a cluster of size $2r$. However if this number r is even (bottom), it can grow and be supplied by the class of clusters $r/2$. Finally since we impose a finite maximum cluster's size n_c, if $r > n_c$, it is not possible for the clusters to grow anymore. Otherwise the resulting cluster $2r$ would exceed the limit n_c. (b) Diagram displaying the case r even and $r > n_c$. We can observe that r can be supplied by the cluster class $r/2$ but cannot grow on order not to exceed the maximum cluster's size n_c.

eq. (32)):

$$\frac{dc_r}{dt} = A_r(t) + K\left(1 - \frac{M(t)}{M_\infty}\right)\begin{cases} \begin{cases} c_1 & r = 1 \\ -c_2 & r = 2 \end{cases} \\ \begin{cases} (c_{r/2} - c_r) & \text{r even} \\ c_{r/2} & \text{r odd} \end{cases} & 2 < r \leq n_c/2 \\ \begin{cases} -c_r & \text{r even} \\ 0 & \text{r odd} \end{cases} & n_c \geq r > n_c/2 \end{cases} \tag{39}$$

The Fig. 14 illustrates with a diagram the meaning of these different equations. For monomers, a bacterium divides and leads to two separated bacteria, it thus increases only c_1. Consequently c_2 does not increase by microbial growth. Then we consider a cluster C_r where all the r bacteria can divide in the same time, which leads to a cluster C_{2r}. This process $C_r \to C_{2r}$ is expressed by the term $-Kc_r$. Furthermore for even r clusters, C_r can also be formed by the microbial growth of a cluster $C_{r/2}$. This process $C_{r/2} \to C_r$ is expressed by the term $+Kc_{r/2}$. Actually, assuming binary division with constant rate for cell reproduction, only even r clusters can be formed by microbial growth.

Furthermore because of the finite maximum cluster's size n_c of the system, a cluster can not be bigger than n_c. This consideration suggests to distinguish the clusters which can double their sizes ($r \leq n_c/2$) from them which can not ($r > n_c/2$), since otherwise they would exceed the limit n_c.

The term $1 - M(t)/M_\infty$ is the exact equivalent as for the logistic model for monomers. When the entire mass of the system achieves the value M_∞ the growth stops, this is the system carrying capacity (see Fig. 13).

4.3.3 Analytical developments

In order to compare with the classical logistic model, we want to find the analytical expression for the mass M(t). For that purpose we determine $\frac{dM(t)}{dt}$. For n_c even :

$$\frac{dM(t)}{dt} = \frac{d}{dt}\sum_{r=1}^{n_c} rc_r = \sum_{r=1}^{n_c} r\frac{dc_r}{dt} \tag{40}$$

$$= \frac{dc_1}{dt} + 2\frac{dc_2}{dt} + \sum_{r=3}^{n_c/2} r\frac{dc_r}{dt} + \sum_{r=n_c/2+1}^{n_c} r\frac{dc_r}{dt} \tag{41}$$

$$= \frac{dc_1}{dt} + 2\frac{dc_2}{dt} + \sum_{p=2}^{n_c/4} (2p)\frac{dc_{2p}}{dt} + (2p-1)\frac{dc_{2p-1}}{dt} + \sum_{p=\frac{n_c+2}{4}}^{n_c/2} (2p)\frac{dc_{2p}}{dt} + (2p-1)\frac{dc_{2p-1}}{dt} \tag{42}$$

$$= K\left(1 - \frac{M(t)}{M_\infty}\right)\left(c_1 - 2c_2 + \sum_{p=1}^{n_c/4}(2p)(c_p - c_{2p}) - (2p-1)c_{2p-1} + \sum_{p=\frac{n_c}{4}+1}^{n_c/2}(2p)c_p + 0\right) \tag{43}$$

$$= K\left(1 - \frac{M(t)}{M_\infty}\right)\left(c_1 - 2c_2 + \sum_{p=2}^{n_c/2}(2p)c_p - \sum_{p=2}^{n_c/4}(2p)c_{2p} + (2p-1)c_{2p-1}\right) \tag{44}$$

$$= K\left(1 - \frac{M(t)}{M_\infty}\right)\left(c_1 - 2c_2 + 2\sum_{r=2}^{n_c/2} rc_r - \sum_{r=3}^{n_c/2} rc_r\right) \tag{45}$$

$$= K\left(1 - \frac{M(t)}{M_\infty}\right)\left(c_1 - 2c_2 + \sum_{r=2}^{n_c/2} rc_r + 2c_2\right) \tag{46}$$

$$= K\left(1 - \frac{M(t)}{M_\infty}\right)\sum_{r=1}^{n_c/2} rc_r \tag{47}$$

Finally:

$$\boxed{\frac{dM}{dt} = K\left(1 - \frac{M(t)}{M_\infty}\right)\left(M(t) - \sum_{r=n_c/2+1}^{n_c} rc_r\right)} \tag{48}$$

Similarly with the case n_c odd we get:

$$\boxed{\frac{dM}{dt} = K\left(1 - \frac{M(t)}{M_\infty}\right)\left(M(t) - \sum_{r=(n_c-1)/2}^{n_c} rc_r\right)} \tag{49}$$

As an exercise we also can find (n_c even):

$$\sum_{r=1}^{n_c} \frac{dc_r}{dt} = \frac{dc_1}{dt} + \frac{dc_2}{dt} + \sum_{r=3}^{n_c/2} \frac{dc_r}{dt} + \sum_{r=n_c/2+1}^{n_c} \frac{dc_r}{dt} \tag{50}$$

$$= \frac{dc_1}{dt} + \frac{dc_2}{dt} + \sum_{p=2}^{n_c/4} \frac{dc_{2p}}{dt} + \frac{dc_{2p-1}}{dt} + \sum_{p=\frac{n_c+2}{4}}^{n_c/2} \frac{dc_{2p}}{dt} + \frac{dc_{2p-1}}{dt} \tag{51}$$

$$= K\left(1 - \frac{M(t)}{M_\infty}\right)\left(c_1 - c_2 + \sum_{p=1}^{n_c/4}(c_p - c_{2p}) - c_{2p-1} + \sum_{p=\frac{n_c}{4}+1}^{n_c/2} c_p + 0\right) \tag{52}$$

$$= K\left(1 - \frac{M(t)}{M_\infty}\right)\left(c_1 - c_2 + \sum_{p=2}^{n_c/2} c_p - \sum_{p=2}^{n_c/4} c_{2p} + c_{2p-1}\right) \tag{53}$$

$$= K\left(1 - \frac{M(t)}{M_\infty}\right)\left(c_1 - c_2 + \sum_{r=2}^{n_c/2} c_r - \sum_{r=3}^{n_c/2} c_r\right) \tag{54}$$

$$= K\left(1 - \frac{M(t)}{M_\infty}\right)(c_1 - c_2 + c_2) \tag{55}$$

Finally:

$$\boxed{\sum_{r=1}^{n_c} \frac{dc_r}{dt} = K\left(1 - \frac{M(t)}{M_\infty}\right) c_1} \tag{56}$$

We get the same solution for the case n_c odd.

4.3.4 Implementation and numerical results

Smoluchowski equations with a multiplicative kernel: $a_{r,s} = rs$: We here consider the same case than in the previous section 4.2, and we add the logistic model for clusters terms.

The addition of the microbial growth phenomenon arises a similar power law behaviour (see Fig. 15(a)). In the classical model c_r follows the law $r^{-5/2}$. The addition of the logistic model for clusters changes this law as $c_r \sim r^{-1.89}$, which is nearer the law we are looking for: r^{-2}.

Without logistic model terms, the mass is conserved as expected (see Fig. 15(b)). The numerical results follow the analytical solution. For short times the mass of the logistic model for clusters follows the classical logistic model. For longer times, the contribution of biggest clusters becomes more important, that is

$$\sum_{r=n_c/2+1}^{n_c} r c_r \tag{57}$$

(see eq. (48)). This term decreases the mass $M(t)$ and represents the difference between the mass evolution for a monomeric or clustered system.

So far we have considered that all the bacteria in a cluster multiply, however we could also consider that in such a biofilm only the bacteria at the surface of a cluster have access to food and place enough to multiply.

4.3.5 Logistic model for bacterial clusters: second equations (growth of the surface)

To determine the number of bacteria at the surface of a cluster, we still consider spherical aggregates. Which involves that the area of a cluster goes as $r^{2/3}$. We modify the former logistic model by

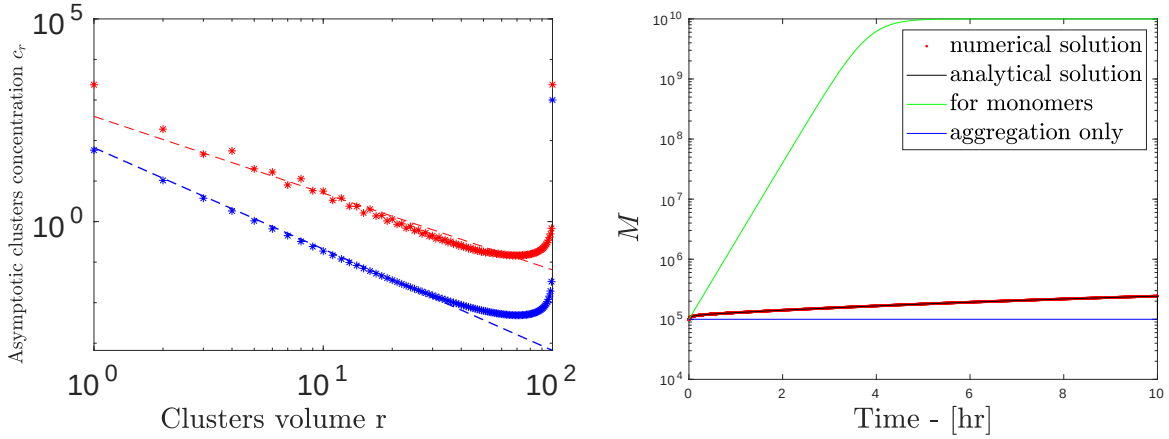

(a) (b)

Figure 15: Numerical simulations for the Smoluchowski model without (blue) or with (red) the logistic model equation eq. (39). (a) Asymptotic clusters concentrations. The straight behaviour with a log-log scale highlights a power law. In the classical model c_r follows the law $r^{-5/2}$. The addition of the logistic model for clusters changes this law as $c_r \sim r^{-1.89}$, which is nearer the law we are looking for: r^{-2}. (b) Temporal mass evolution. Without logistic model terms (blue line), the mass is conserved as expected. The numerical results (red line) follow the analytical solution (black line). For short times the mass of the logistic model for clusters follows the classical logistic model (green line). For longer times the contribution of biggest clusters becomes more important, which explains the difference between the model for monomers and clusters (see eq. (48)).

considering that for the clusters bigger than a characteristic size T_c only the bacteria at the surface can multiply (we consider $T_c < n_c/2$). However smaller clusters still grow following the previous equations (eq. (39)), that is every bacterium divides.

$$\frac{dc_r}{dt} = A_r(t) + K\left(1 - \frac{M(t)}{M_\infty}\right)\begin{cases} \begin{cases} c_1 & r = 1 \\ -c_2 & r = 2 \end{cases} & \\ \begin{cases} (c_{r/2} - c_r) & \text{r even} \\ c_{r/2} & \text{r odd} \end{cases} & 2 < r \leq 2T_c \\ \begin{cases} (c_{r-r^{2/3}} - c_r) & r \leq n_c - n_c^{2/3} \\ c_{r-r^{2/3}} & r > n_c - n_c^{2/3} \end{cases} & n_c \geq r > 2T_c \end{cases} \tag{58}$$

We observe a similar consequence on clusters concentrations (see Fig. 19 in Annexes), but with a slightly different value of the power, which is not $-5/2$ anymore. This value changes depending on the value of T_c. For the highest value of $T_c = \lfloor n_c/2 \rfloor$, we get a power -1.93, which is nearer the one we search to model: -2.

We finally have found a model which is physically consistent and allows to model the experimental distribution of clusters sizes, which was our starting point. Finally we will study what impact on the kinetics of Mn have these clusters of bacteria.

5 Impact on the kinetics of Mn

5.1 A kinetic equation for the mineralisation of Mn by clustered bacteria

As a first approximation the kinetics of the mineralisation of Mn can be considered as a first-order reaction [4] [5]. In case of separated bacteria (monomers), we write:

$$\frac{dc_M}{dt} = -K_m c_1 c_M(t) \tag{59}$$

Where c_1 is the concentration of bacteria (monomers), c_M refers to the concentration of Mn in $[g.mL^{-1}]$, K_m is the reaction rate constant, its unit is $[t^{-1}]$. However we here also consider the clustering process between bacteria. This phenomenon implies a different K_m for each cluster's size, since only the bacteria at the surface of a cluster can react and catalyse with the Mn elements. That is why we write:

$$\frac{dc_M}{dt} = -\left(\sum_{r=1}^{n_c} K_r c_r\right) c_M(t) \qquad \text{with} \qquad K_r = r^{2/3} K_m, \quad \forall r > 1 \tag{60}$$

since we consider spherical aggregates, the surface goes as $A \sim r^{2/3}$, where r represents both the volume and the number of monomers.

5.2 Analytical solutions for the concentration of Mn (Smoluchowski model)

We study this equation for the case of the Smoluchowski model with a multiplicative kernel $a_{r,s} = rs$ (see section 4.2), since it is the best model we have found. Firstly, we can characterise analytically c_M. We distinguish the cases $t < t_g = 1$ and $t > t_g = 1$ (see eq (36)).

For $t < t_g = 1$:

$$\frac{dc_M}{dt} = -\left(\sum_{r=1}^{n_c} K_m r^{2/3} c_r\right) c_M(t) \tag{61}$$

$$= -\left(\sum_{r=1}^{n_c} K_m r^{2/3} \frac{1}{t\sqrt{2\pi}} r^{-5/2} e^{-r(t-1-log(t))}\right) c_M(t) \tag{62}$$

$$= -\frac{K_m}{\sqrt{2\pi}}\left(\sum_{r=1}^{n_c} r^{2/3-5/2} e^r e^{-rt} t^{r-1}\right) c_M(t) \tag{63}$$

We write:

$$I_r(t) = \int_0^t du\ e^{-ru} u^{r-1} \tag{64}$$

After a change of variables $v = ru$ we get:

$$I_r(t) = \int_0^t \frac{dv}{r}\ e^{-v} \frac{v^{r-1}}{r^{r-1}} = r^{-r} \int_0^t dv\ r e^{-v} v^{r-1} = r^{-r}\gamma(r,t) \tag{65}$$

Where $\gamma(r,t)$ is the lower incomplete gamma function. Finally:

$$\boxed{c_M(t) = c_M(t=0) exp\left(-\frac{K_m}{\sqrt{2\pi}}\left(\sum_{r=1}^{n_c} r^{2/3-5/2-r} e^r \gamma(r,t)\right)\right), \qquad t < t_g = 1} \tag{66}$$

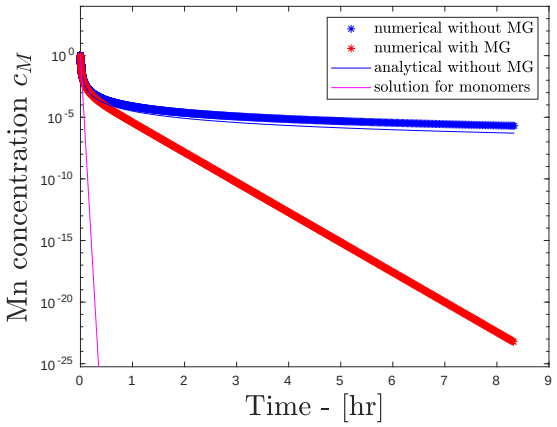

Figure 16: Numerical simulations of the temporal evolution of the concentration of Mn in presence of clustered bacteria. We used the Smoluchowski equations (see section 4.3) to model the microbial clusters distribution, without or with the microbial growth. The red dots represent numerical results, the magenta line refers to a solution for bacterial monomers $c_M(t) = c_M(t=0)exp(-Kmt)$. The blue line corresponds to the analytical solution (66), (71), for the case without microbial growth. Without microbial growth, numerical results follow the analytical solution. When microbial growth is taken into account, the distribution seems to be exponential, but with a different exponent than for the classical case for monomers.

For $t > t_g = 1$:

$$\frac{dc_M}{dt} = -\left(\sum_{r=1}^{n_c} K_m r^{2/3} c_r\right) c_M(t) \tag{67}$$

$$= -\left(\sum_{r=1}^{n_c} K_m r^{2/3} \frac{1}{t\sqrt{2\pi}} r^{-5/2}\right) c_M(t) \tag{68}$$

$$= -\frac{K_m}{\sqrt{2\pi}}\left(\sum_{r=1}^{n_c} r^{2/3-5/2}\right)\frac{1}{t}\, c_M(t) \tag{69}$$

$$= -f(r)\frac{1}{t}c_M(t) \tag{70}$$

Then

$$\boxed{c_M(t) = c_M(t=t_g)(t/t_g)^{-f(r)} \quad \text{with } f(r) = \frac{K_m}{\sqrt{2\pi}}\left(\sum_{r=1}^{n_c} r^{2/3-5/2}\right), \quad t > t_g = 1} \tag{71}$$

5.3 Implementation and numerical results

In Fig. 16 we observe that without microbial growth, numerical results follow the analytical solution. When microbial growth is taken into account, the distribution seems to be exponential, but with a different exponent than for the classical case for monomers.

Finally it seems that bacterial clustering slows the decrease of the Mn concentration c_M, that is the mineralisation process. On the opposite the microbial growth process seems to fast the speed of the reaction.

6 Conclusion

6.1 Models to explain the dynamics of bacteria aggregation

Starting from experimental data, we have developed different models to characterise the observed experimental distribution of clusters areas. Considering spherical aggregates, we showed that the distribution law $c_A \sim A^{-\alpha_A}$, corresponds to $c_r \sim r^{-(2\alpha_A+1)/3} = r^{-\alpha_r}$. The experimental distribution gives $\alpha_r \sim 2$. Both Smoluchowski and Becker-Döring equations allow to model power laws following the desired distribution. However, the most physically sound model which allows to retrieve the expected distribution is the Smoluchowski model with a multiplicative kernel and considering microbial growth.

The kinetics of precipitation of Mn is modified depending on two distinct considerations: if bacteria are separated or organised in clusters, and if microbial growth is taken into account. It seems that bacterial clustering slows the decrease of the Mn concentration, that is the mineralisation process. On the opposite the microbial growth process seems to fast the speed of the reaction.

6.2 A model to explain the formation of porous media

On the other hand we have developed analytical solutions for the Becker-Döring model, leading to the aggregate size concentration c_r following Gamma distributions. Interestingly for porous media, it has been observed that the distribution of the pores sizes also follows a Gamma distribution. That is why we could suggest that the formation of porous media is made via a process which could be modelled by the Becker-Döring equations (following the conditions we determined). In fact instead of considering bacteria for our elementary particles, it could be grains of sand which would be progressively deposited on the medium in formation. This progressive deposit would justify the use of a model considering aggregation-fragmentation processes only with the gain or the loss of a single particle.

6.3 Limits and perspectives

The model we developed could be improved on some points. Firstly the way we define the equations of the logistic model for clusters could be more precise, in order to better model the suspected physical phenomenon. Secondly, it would be interesting to continue to study the kinetics of Mn in presence of microbial aggregates, since bacteria can be organised in clusters in the soil.
Then, the link between the Becker-Döring model and the formation of porous media could be investigated more in depth.
Furthermore, we have considered so far that aggregates had a spherical shape. Nevertheless this hypothesis could be challenged out, further studies could be focused on determining the precise shape of such bacterial aggregates.
Finally it is also interesting to point out the fact that the suitable kernels are of the form $a_r = a_0 r^\alpha$, where α could characterise a physical phenomenon. It should be interesting to investigate this fact into more details.

7 Annexes

7.1 Becker-Döring model and microbial growth:

We add the logistic model terms, as for the Smoluchowski model, to the Becker-Döring model for a steady-state and $a_r = a_0 r^\alpha$, $b_r = b_0 r^\alpha$.

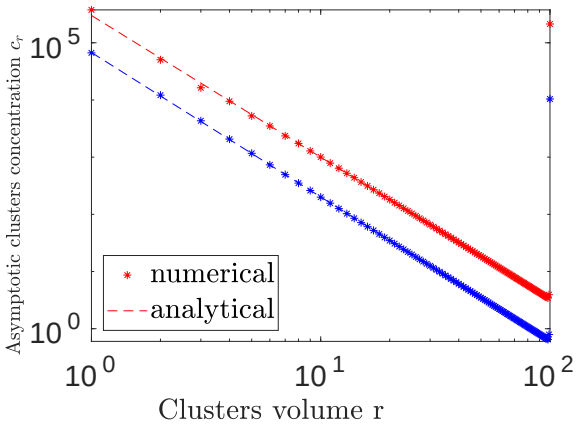

Figure 17: Numerical simulations for the Becker-Döring model without (blue) or with (red) the logistic model. $\alpha = 5/2$. Numerical values α_N are very near the exact value 5/2.

We observe a similar behaviour between the situation with or without logistic model terms. The only difference lays in the total mass of the system, which rises the values of clusters concentrations when microbial growth is considered.

7.2 Smoluchowski model with fragmentation, constant kernels: $a_{r,s} = a_0$, $b_{r,s} = b_0$.

Firstly, as a test to verify if the equations have been correctly implemented, we focus on this particular case with constant kernels for which an exponential distribution is expected at equilibrium.

Remark: The equilibrium state, $\forall r, W_{r,s} = 0$, should be distinguished from the steady-state, which is the general case $\forall r$, $\frac{dc_r}{dt} = 0$. In this research project, in order to discriminate for numerical results whether a state is equilibrium or steady-state, we compare the minimum of $\frac{dc_r}{dt}$ and $\sum_{r=1}^{n_c} W_{r,s}$ with a threshold value ϵ. If the condition $\min(\frac{dc_r}{dt}, \sum_{r=1}^{n_c} W_{r,s}) < \epsilon$ is satisfied, that means that the state would be at equilibrium (if $\min = \sum_{r=1}^{n_c} W_{r,s}$) or steady ($\min = \frac{dc_r}{dt}$).

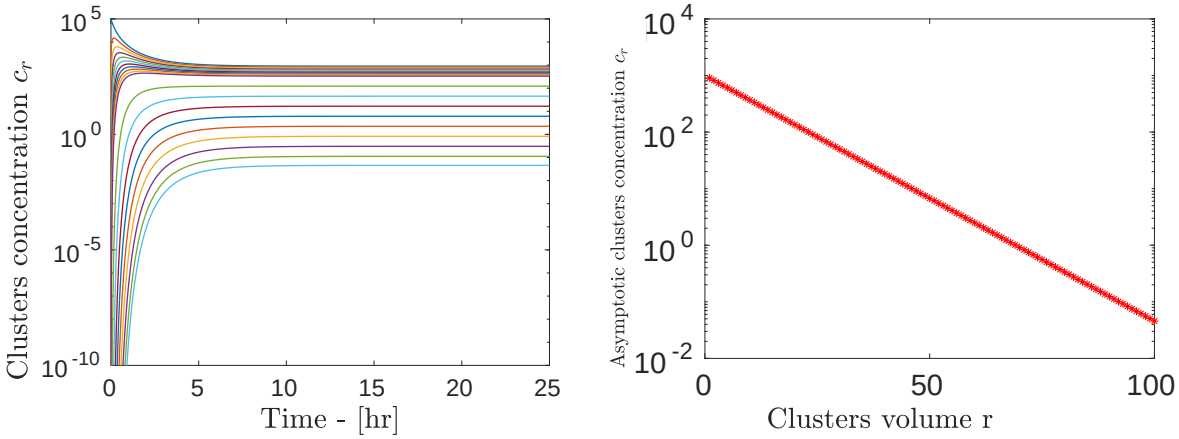

(a) (b)

Figure 18: Numerical simulation of the Smoluchowski model with kernels $a_{r,s} = a_0$, $b_{r,s} = b_0$. (a) Temporal evolution of each cluster's size, (b) Asymptotic clusters concentration c_r. The straight behaviour with the semi-log scale highlights an exponential decay

The straight behaviour with a semi-log scale plot highlights an exponential decay, which is consistent with the expected calculated results of our reference article [1]. This confirms that the model has been correctly implemented.

We then move onto models which could fit the experimental distribution we get.

7.3 Analytical kernels for the Smoluchowski equations

Our aim is to find parameters, especially kernels $a_{r,s}$, $b_{r,s}$, in order to get $c_r \sim r^{-\alpha}$, with $\alpha = 2$. Starting from this, and considering an equilibrium state, that is

$$W_{r,s} = 0 \tag{72}$$

By substituting $c_r = c_1 r^{-\alpha}$ we have

$$a_{r,s} c_1 r^{-\alpha} s^{-\alpha} = b_{r,s}(r+s)^{-\alpha} \tag{73}$$

We find a trivial solution for the aggregation and fragmentation rates:

$$\begin{cases} a_{r,s} = a_0 (rs)^{\alpha} \\ b_{r,s} = b_0 (r+s)^{\alpha} \\ a_0 c_1 = b_0 \iff \theta = 1 \end{cases} \tag{74}$$

These conditions on kernels should allow to get a power law distribution of clusters volumes $c_r \sim r^{-\alpha}$. Nevertheless we do not have a way to determine exactly the equilibrium value of c_1, that is why we do not succeed in obtaining a numerical confirmation of this calculation.

7.4 Smoluchowski model and microbial growth at the surface of clusters

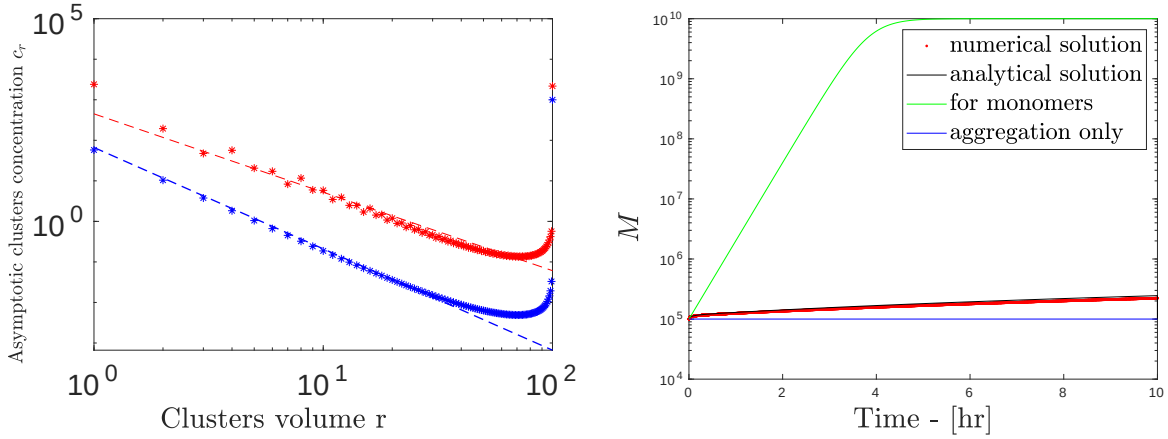

(a) (b)

Figure 19: Numerical simulations for the Smoluchowski model without (blue) or with (red) the logistic model equation eq. (58).(a) Asymptotic clusters concentrations. The straight behaviour with a log-log scale highlights a power law. In the classical model c_r follows the law $r^{-5/2}$. The addition of the logistic model for clusters changes this law as $c_r \sim r^{-1.93}$, which is nearer the law we are looking for: r^{-2}. (b) Temporal mass evolution. Without logistic model terms (blue line), the mass is conserved as expected. The numerical results (red line) follow approximately the analytical solution determined for the previous equation 39 (black line). For short times the mass of the logistic model for clusters follows the classical logistic model (green line). For longer times the contribution of biggest clusters becomes more important, which explains the difference between the model for monomers and clusters (see eq. (48)).

References

[1] Jonathan A.D. Wattis, "An introduction to mathematical models of coagulationâfragmentation processes: A discrete deterministic mean-field approach", *Physica*, **Volume 222** , 1-20 (2006).

[2] Ricardo I. Jeldresa, Phillip D. Fawell, Brendan J. Florio, "Population balance modelling to describe the particle aggregation process: A review", *Powder Technology*, **Volume 326** , 190-207 (2018).

[3] Réka Albert and Albert-László Barabási, "Statistical mechanics of complex networks", *Reviews of Modern Physics*, **Volume 74** (2002).

[4] Peter J. Von Langen, Kenneth S. Johnson, Kenneth H. Coale, and Virginia A. Elrod, "Oxidation kinetics of manganese (II) in seawater at nanomolar concentrations", *Geochimica et Cosmochimica Acta*, **Volume 61** , 4945-4954 (1997).

[5] James J. Morgan, "Kinetics of reaction between O2 and Mn(II) species in aqueous solutions", *Geochimica et Cosmochimica Acta*, **Volume 69** , 35-48 (2005).

[6] Colm Connaughton, R. Rajesh, Oleg Zaboronski, "Stationary Kolmogorov Solutions of the Smoluchowski Aggregation Equation with a Source Term", *hal-00000669v2*,(2004).

[7] T. Birnstiel, C. W. Ormel, and C. P. Dullemond, "Dust size distributions in coagulation/fragmentation equilibrium: numerical solutions and analyticalal fits",*Astronomy & Astrophysics* **Volume 525, A11** ,(2011).

[8] Papoulis, Pillai, "Probability, Random Variables, and Stochastic Processes, Fourth Edition", (2002).

[9] Michael T. Madigan, Kelly S. Bender, Daniel H. Buckley, W. Matthew Sattley, David A. Stahl, "Brock Biology of Microorganisms (15th Edition)", (2017).

[10] Tomasz Michal Trzeciak, "Brownian coagulation at high particle concentrations", (2012).